International Journal of Applied Science and Engineering
2009. 6, 3: 215-221

Characterizing the performance of eddy current probes using photoinductive field-mapping: a numerical approach

Cheng-Chi Tai, Yen-Lin Pan*

Department of Electrical Engineering,National Cheng Kung University

Abstract: Nondestructive evaluation (NDE) method has been applied to analyze the configurations of coil probes and the characteristics of discontinuities in the few years, especially the effects of probe tilt are paid attention to gradually. However, the probe tilt has been recognized as the one reason of producing noise in eddy current testing (ECT), such as the flaw manual scanning or the manufacture of probes with the irregular orientation coil. The inability to calibrate the tilt coil of probe makes it impossible to accurately inspect the surface cracks. Based on the above, we should found the applicable method to examine the structures of probe and demonstrate that it has the feasibility on investigating of probe with tilted coil. The photoinductive (PI) method is a novel inspection technique for detecting surface cracks. This paper shows how the PI technique can be utilized to analyze the effects of tilted coil of probe. The numerical multiphysics simulations of the PI imaging was performed with two dimensional finite element method (2D FEM) to characterize the variations of magnetic field and probe's impedance on a conductive metal foil. As anticipated, the proposed model shows that the PI imaging signals can reveal the construction of the probe. The FEM simulation results of tilted coils are showed and discussed. The effects of PI signals with different excited frequencies of the coil are also examined and analyzed. The simulation results demonstrate that not only the PI method is appropriate for investigating the structures of probe, but also how the tilt probe can affect the reliability of an eddy current inspection.

Keywords: coil tilt; eddy current testing (ECT); finite element method (FEM); nondestructive testing (NDT); photoinductive imaging (PI).

1. Introduction

The characterization of the performance of eddy current (EC) probes is important problem in NDE. The magnetic field intensity of the EC probe and the EC density within the material are necessary to observe for calibrating the tilted EC probes. Many researchers have studied the problem of eddy current induction by a tilted coil above a planar conductor [1]-[6]. The calculation of eddy currents within a conducting plate when the excitation is a circular current loop with a tilted angle was examined [1]. The photoinductive method supplants the use of artifact standards to calibrate eddy current probes and maps the magnetic field of the eddy current probe. Furthermore, the probe's field pattern reveals defects in probe construction [2]. An analytical EC model was built and computed the

* Corresponding author; e-mail: cati666@gmail.com
Accepted for Publication: April 10, 2009

fields induced in the case of an elementary wire above a half-space or a plate by current sources of arbitrary orientation [3]. The electromagnetic field and impedance of a cylindrical eddy-current probe coil are calculated analytically for arbitrary coil orientation above a conductive half-space [4]. A numerical simulation with a tilted coil is investigated in external eddy current inspection of tubes [5] and in electromagnetic-thermal nondestructive inspection of conductive plates [6].

The photoinductive (PI) method overcomes the disadvantages of previous eddy current probe field-mapping techniques, such as large probe size, poor signal to noise ratio, or insensitivity to the tangential component of the magnetic field [2]. Therefore, we apply the finite element method to simulate this technique in this paper and to map eddy current probes with different tilted angles of the coil. The physical principles and basic formulas are described briefly. The proposed model calculates the magnetic field and probe's impedance above a metal foil. Based on the simulation results, we also discuss the effect of tilted angle and excited frequency of the coil.

2. The photoinductive method

Figure 1 illustrates the physical principles of the PI method. The probe with a cylindrical air cored coil is placed in close proximity to a conductive metal foil and excited with sufficient voltage and at the desired frequency. When the laser beam is focused on the specimen surface from below, the temperature fluctuation causes variations in the electrical conductivity of the metal foil, which in turn, induces a change in the impedance of the probe. The electrical conductivity of the metal foil is given by the expression:

$$\sigma = \frac{1}{[\rho_0(1+\alpha(T-T_0))]} \quad (1)$$

where ρ_0 is the resistivity at temperature T_0, and α is the temperature coefficient of the resistivity. T_0 is the temperature 293 K, and T is the actual temperature in the metal foil sub-domain.

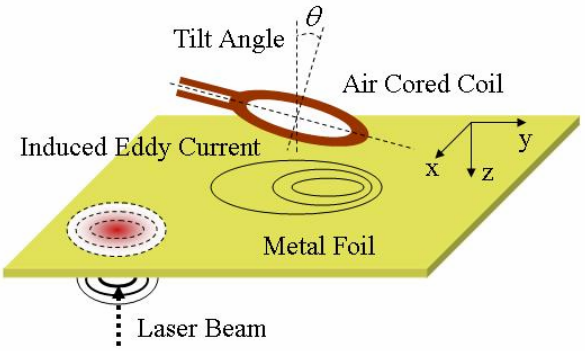

Figure 1. Schematic diagram of photoinductive field mearsurement.

The PI effect can be calculated as follows. The dependent variable in this application mode is the azimuthal component of the magnetic vector potential, $\mathbf{A}$, which conforms to the following relation:

$$(j\omega\sigma - \omega^2\varepsilon)\mathbf{A} + \nabla\times(\mu^{-1}\nabla\times\mathbf{A}) = \frac{\sigma V_{loop}}{L} \quad (2)$$

where ω denotes the angular frequency, σ the conductivity, μ the permeability, ε the permittivity, L the length, and V_{loop} the voltage applied to the coil. The conductivity outside the coil is zero. According to the constitutive relation (*C.R.*), the current density $\mathbf{J}^e$ and magnetic field intensity $\mathbf{H}$ can be calculated as follows.

$$\mathbf{J}^e = \sigma\mathbf{E} = -\sigma(\nabla V + \frac{\partial\mathbf{A}}{\partial t}) \quad (3)$$

$$\mathbf{H} = \frac{\mathbf{B}}{\mu} = \frac{\mathbf{B}}{\mu_0\mu_r} = \frac{\nabla\times\mathbf{A}}{\mu_0\mu_r} \quad (4)$$

where $\mathbf{E}$ and $\mathbf{B}$ denote the electric field inten-

sity and magnetic flux density. μ_0 and μ_r are permeability of free space and relative permeability. The electric potential V is obtained from Faraday's law.

The defining equation for the magnetic vector potential **A** is a direct consequence of the magnetic Gauss' law. The induced current I in the coil is calculated by the integration of current density in the cross-sectional area **s** of the coil. Ohm's law is finally used for calculating the impedance of the probe. The induced current includes real and imaginary components, as shown in Eq. (6).

$$\int_{\mathbf{s}} \mathbf{J}^e \cdot d\mathbf{s} = I \tag{5}$$

$$Z = \frac{V_{loop}}{I} = \mathrm{Re}\{Z\} + \mathrm{Im}\{Z\} \tag{6}$$

The temperature in the z direction of the foil with virtually no diffusion is assumed to be penetrated by the thermal energy of the laser beam source. The temperature, T, is uniformly distributed over the x and y directions of the foil. The mathematical model for heat transfer by conduction is as follows:

$$\rho C \frac{\partial T}{\partial t} + \nabla \cdot (-k \nabla T) = Q \tag{7}$$

where T, ρ, C, k, and Q are the temperature, density, heat capacity, thermal conductivity, and heat source, respectively. In our experiments, applying the weak constraint produced the solutions of Eq. (7) on the laser point temperature so the heat source Q is zero. The specimen properties are considered independent of temperature and constant heating time of the order of one second.

3. Simulated Parametric Study

In this paper, we assume that the eddy current probe is constructed from a cylindrical air cored coil and use the 2D model for solving the 3D problem of a tilted coil above a conductive metal foil, as shown in Figure 2. The rectangular coordinate system is used in this paper. The metal foil with dimensions 10 mm x 10 mm and thickness 10 μm lies on the x-y plane. The coil axis parallels the z-axis and is tilted through an angle θ with respect to the surface normal of metal foil. The air cored copper coil (inner radius r_1 = 0.4 mm ,outer radius r_2 = 1.2 mm, and lift-off distance d = 0.2 mm) is excited is excited with 5-V ac current and 2-MHz, 200-kHz, or 20-kHz frequency. The metal foil is a conductive material with resistivity at temperature 293 K ρ_0 = 2.4x10^{-8} Ω-m, temperature coefficient of the resistivity α = 3.24 x10^{-3} 1/K, density ρ = 4940 kg/m^3, heat capacity C = 710 J/kg-K and thermal conductivity k = 7.5 W/m-k. The temperature of laser beam point is 573 K. In the 2D raster scan simulations, the probe was fixed on the center of the metal foil, while the laser point was moved along the y-axis. It is interesting to observe that the magnetic field intensity of all subdomain space, the current density within the metal foil, and the impedance of the probe. The commercial FEM software, COMSOL Multiphysics™, was utilized in solving the 2D model in this work.

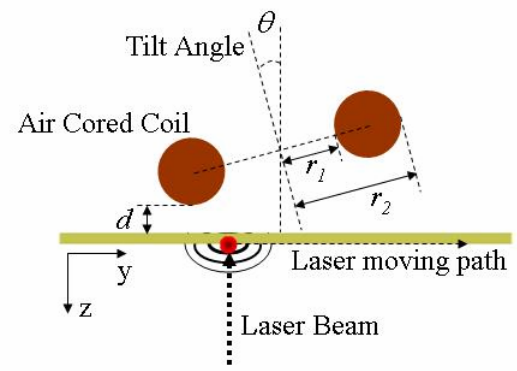

Figure 2. Tilted air-cored cylindrical coil above the metal foil. The cross sectional view shows the x=0 plane.

4. Results

Figures 3 and 4 show streamlines, flow directions and distributions of magnetic field in

free-space at 0^o and 60^o tilt angles. The excited frequency of the probe is 2 MHz in Figures 3-8. The magnetic field intensity can be calculated from Eq. (4). For a parallel coil ($\theta = 0^o$), magnetic field flows symmetrically while for the tilted coil streamlines are asymmetrical and flows tend to either sides of the coil faces. We note that the maximum value of magnetic field intensity for the tilted coil has a raise form comparing to the parallel one. As expected in Figure 5, eddy current density is stronger on the side where the coil is closer to the metal foil. Figure 5 shows the x-component of the current density induced within the foil by the coil probe. The coil is placed above the foil center at various inclination angles. The dual peak values within a region corresponding nearly to the projection of the coil section on the foil when $\theta = 0^o$. Furthermore, the positive peak value indicates the current flow inside the coil section, and the negative peak value is in the opposite situation. The current density decreases for intermediate angles of inclination, such as $\theta = 20^o$ or 40^o, while for 60^o it takes its peak value near the foil center.

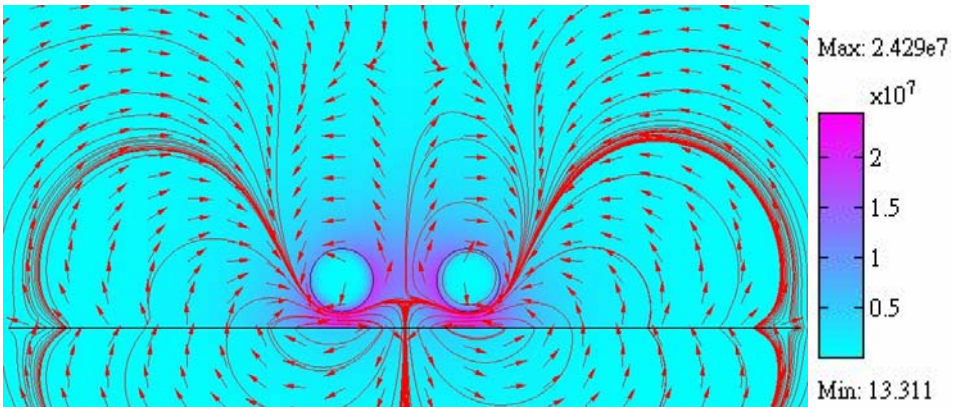

Figure 3. Streamlines, flux directions and distributions of magnetic field induced in free-space by an air-cored cylindrical coil at 0^o tilt angles.

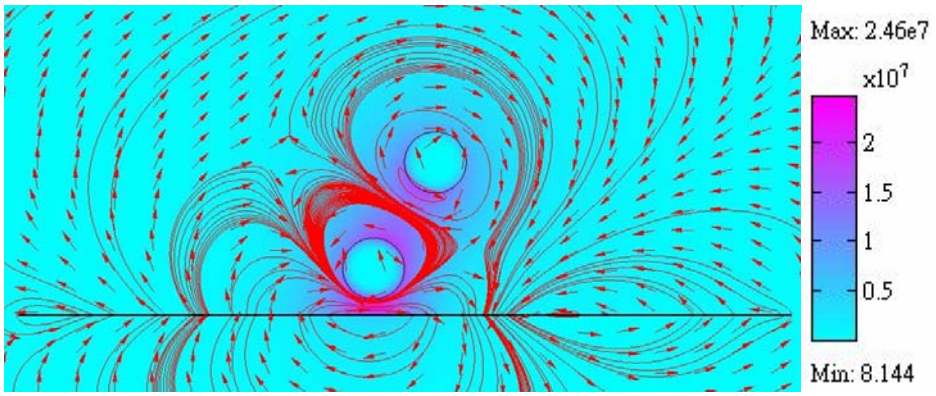

Figure 4. Streamlines, flux directions and distributions of magnetic field induced in free-space by an air-cored cylindrical coil at 60^o tilt angles.

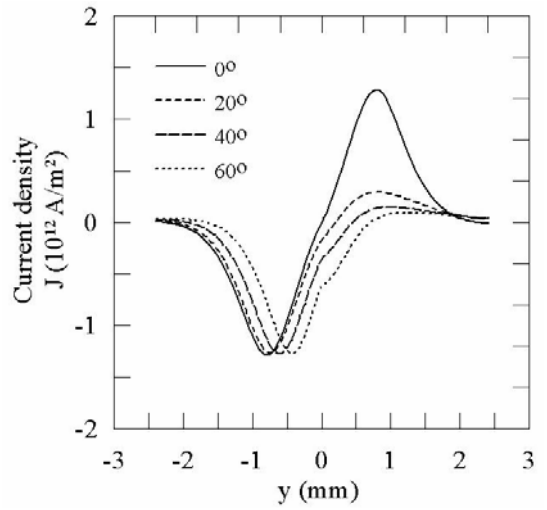

Figure 5. Variation of the x-component of the current density induced within the foil by the coil probe for various inclination angles.

The phase discrimination technique is applied commonly by rotating the impedance display in ECT. The constant phase signal is produced by any change of coil tilt orientation [4]. From Figure 6 we observe that the phase curves are almost straight lines, but higher degree of phase when the tilted angle is increased. Different phase signals indicate the change of another parameter such as the variation of σ or μ_r affected by laser temperature or the presence of a flaw.

In Figures 7 and 8, it can be observed that the resistance and reactance components of impedance change for different tilted angles of the coil. The obliquity of probe is the significant parameter influencing the response of the resistance and reactance components. For $\theta = 0^o$, a double peak values are symmetrical in both components. However, increasing the coil inclination shifts the peak value of resistance or reactance component to the center of the foil. The common relation found between the magnitude of both components and the tilt angle is nonlinear. As far as the inclination angle of the coil is concerned, the tilt curves are compared with three distinct frequencies in Figures 9 and 10, which plot normalized resistance or reactance component versus inclination angle. The impedance is normalized in usual ECT. Moreover, R_0 and X_0 are resistance and reactance components of coil impedance when the laser spot is at the starting point. As shown in Figure 9, the decrease of resistance with tilted angle due to the weaker electromagnetic coupling of the coil with the metal foil. However, the reactance is increased in Figure 10. Using higher frequency is more sensitive to the coil inclination when compared with lower frequency. A minimum in normalized resistance component is at $\theta = 60^o$, although the maximum in normalized reactance component is around 60^o, 30^o and 10^o corresponding to 2 MHz, 200 kHz and 20 kHz, respectively.

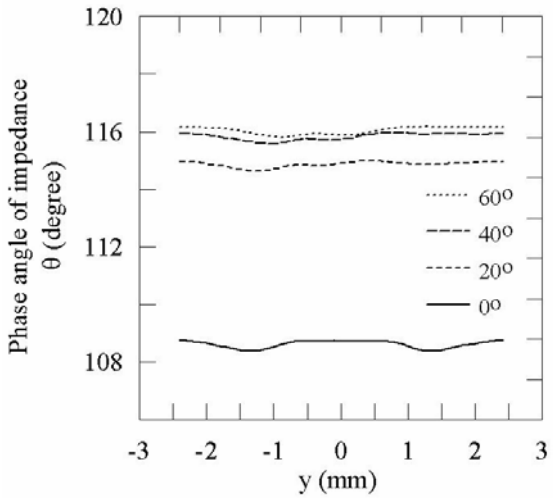

Figure 6. The phase angle of impedance for different coil inclination angles.

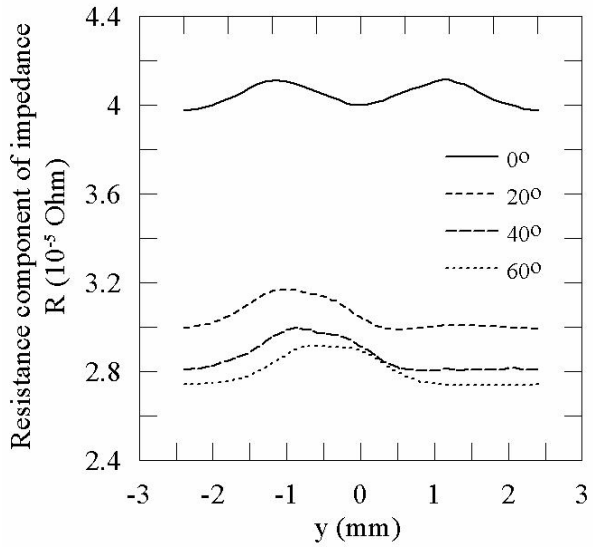

Figure 7. The resistance component of impedance for varying coil obliquity.

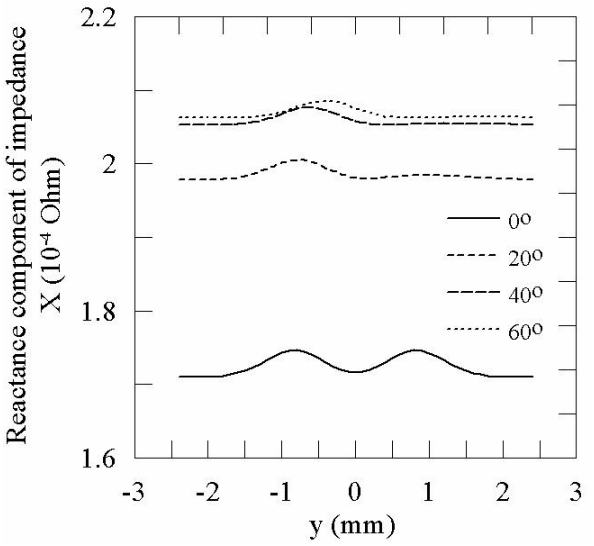

Figure 8. The reactance component of impedance for varying coil obliquity.

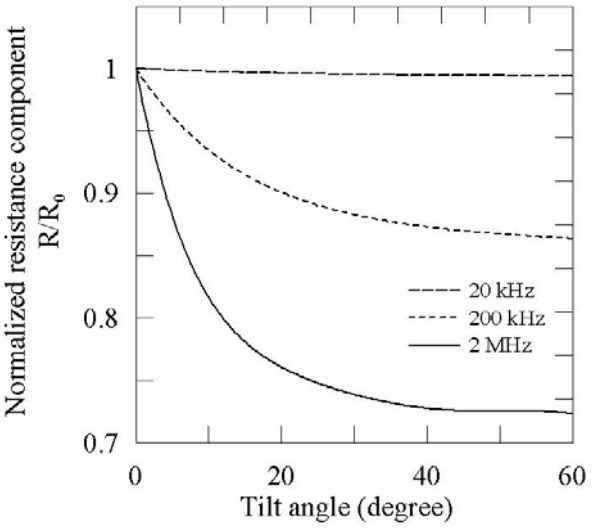

Figure 9. Normalized resistance component of the impedance variation versus inclination angle.

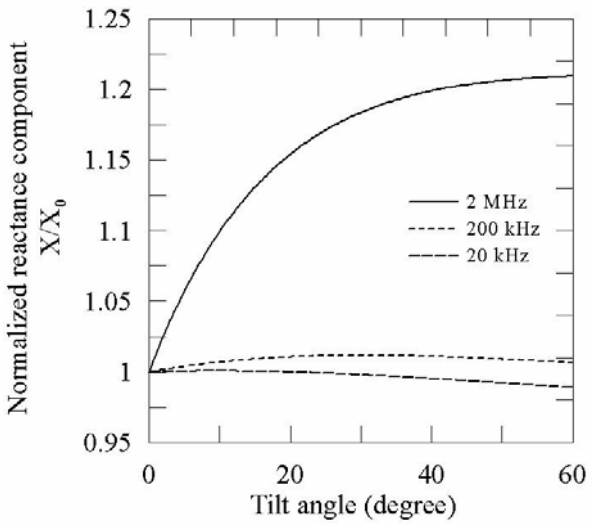

Figure 10. Normalized reactance component of the impedance variation versus inclination angle.

5. Conclusions

The FEM simulation results demonstrate the appropriateness of photoinductive method when applied to characterize and calibration of the eddy current probes with a tilted coil. Increasing tilted angle of the coil causes the phase angle and the reactance component of the coil impedance to rise, but the resistance component is decreased. The impedance of coil using lower frequency is more insensitive to the tilted angle of the coil. Therefore, the excited frequency of the coil should be as high as possible for characterizing the structure of EC probes with a tiled coil. Besides, the small amplitude of resistance component at large frequency, while the large amplitude of resistance component at the same frequency.

6. Acknowledgements

This research was supported by the grant from National Science Council, Taiwan (NSC 96-2628-E-006-256-MY3). Also, this work made use of Shared Facilities supported by the Program of Top 100 Universities Advancement, Ministry of Education, Taiwan.

References

[1] Tsaknakis, H. J., and Kriezis, E. E. 1985. Field Distribution Due to a Circular Current Loop Placed in an Arbitrary Position above a Conducting Plate, *IEEE Transactions on Geoscience and Remote Sensing,* GE-23: 197-207.

[2] Moulder, J. C., and Nakagawa, N. 1992. Characterizing the performance of eddy current probes using photoinductive field-mapping, *Research in Nondestructive Evaluation*, 4: 221-236.

[3] Juillard, J., de Barmon, B., and Berthiau, G. 2000. Simple analytical three-dimensional eddy-current model, *IEEE Transactions on Magnetics*, 36: 258-266.

[4] Theodoulidis, T. 2005. Analytical model for tilted coils in eddy-current nondestructive inspection, *IEEE Transactions on Magnetics*, 41: 2447- 2454.

[5] Reboud, C., Prémel, D., Pichenot, G., Lesselier, D., and Bisiaux, B. 2005. Development and validation of a 3D model dedicated to eddy current non-destructive testing of tubes by encircling probes, *Proceedings on 12th International Symposium on Interdisciplinary Electromagnetic, Mechanic and Biomedical Problems*, 278-279.

[6] Tsopelas, N., and Siakavellas, N. J., 2007. The effect of the angle of inclination of the exciting coil in electromagnetic-thermal non-destructive inspection, *Proceedings of the 4th International Conference on Non-Destructive Testing*.